



Preliminary Design of the Flight Control System for a Mach 5 Hypersonic Civil Passenger Aircraft

Oscar Gori¹, Simona Loccisano², Davide Ferretto³, Nicole Viola⁴

Abstract

The Flight Control System (FCS) plays a crucial role in enabling the maneuverability and stability of the aircraft across a wide range of flight conditions. It is of utmost importance to consider the FCS during the initial stages of a project, particularly when designing high-speed vehicles, where the impact of control surfaces deflections on the aerodynamic performance may be significant. Additionally, ensuring high-speed aircrafts' maneuverability and stability while meeting required standards presents a greater challenge compared to conventional subsonic aircraft. This paper addresses the preliminary design of the flight control system for a hypersonic aircraft: the STRATOFly MR5, a Mach 5 civil passenger vehicle developed within the H2020 MORE&LESS project. The steps followed in the preliminary design of the flight control system are reported. Initially, the geometric definition of all control surfaces is presented, followed by an estimation of potential deflections required to achieve vehicle's stability and trim along the different flight regimes.

Keywords: *Hypersonic Civil Aircraft, Flight Control System Design*

Nomenclature

AR_c	– Canard Aspect Ratio	MAC	– Mean Aerodynamic Chord
b_c	– Canard span	$MTOM$	– Maximum Take-Off Mass
C_{M_y}	– Pitching moment coefficient	S_c	– Canard plan surface
CoG	– Centre of Gravity	S_{ref}	– Vehicle reference surface
c_{r_c}	– Canard root chord	x_{ac}	– Aerodynamic center
c_{t_c}	– Canard tip chord	x_{CoG}	– Position of the center of gravity
C_z	– Lift coefficient	V_c	– Canard surface volume coefficient
FCS	– Flight Control System	α	– Angle of attack
l_c	– Canard arm with respect to center of gravity	Λ_c	– Canard sweep angle
		λ_c	– Canard taper ratio

1. Introduction

After the discontinuation of civil supersonic flight with Concorde in 2003, various projects aimed at reviving high-speed air travel have emerged. One such project is STRATOFly, which received funding from the European Union's Horizon 2020 program and explored the feasibility of high-speed passenger stratospheric flight [1]. The STRATOFly MR3 vehicle, which is designed for Mach 8 flight, is the main outcome of this project.

The European Commission is currently funding the H2020 MORE&LESS project [2], which aims to help Europe influence global environmental regulations for future supersonic aviation. This project encompasses a wide range of supersonic speeds, from Mach 2 to Mach 5, and includes aircraft using alternative fuels like biofuels and liquid hydrogen. As part of MORE&LESS, the MR5 concept, a Mach 5 civil passenger aircraft, has been selected for analysis, building upon the findings of the H2020 STRATOFly project.

¹ Politecnico di Torino, Corso Duca degli Abruzzi, 24, Torino, Italy, oscar.gori@polito.it

² Politecnico di Torino, Corso Duca degli Abruzzi, 24, Torino, Italy, s271623@studenti.polito.it

³ Politecnico di Torino, Corso Duca degli Abruzzi, 24, Torino, Italy, davide.ferretto@polito.it

⁴ Politecnico di Torino, Corso Duca degli Abruzzi, 24, Torino, Italy, nicole.viola@polito.it

This paper presents the methodology used to perform the preliminary design of the MR5 Flight Control System (FCS), starting from the geometrical definition of control surfaces and later focusing on vehicle's longitudinal static stability and trim. Flight control surfaces are fundamental to properly maneuver and trim the aircraft in each flight condition. These capabilities, and the stability of the vehicle, are much influenced by the positions of center of gravity (CoG) and aerodynamic center [3]. Moreover, it should also be considered that, for the specific case of high-speed systems, the position of these two points can vary significantly during the different flight regimes. The shift of the CoG is mainly influenced by fuel consumption and tanks depletion strategy adopted. Furthermore, the aerodynamic center also shifts through the different flight regimes. Hence, it is possible to highlight the importance of a high integration among on-board subsystems, which is another typical aspect of high-speed vehicles. First, it could be advantageous to define a proper depletion strategy for the fuel system to control the CoG's shift. Moreover, the avionic system can be designed to solve stability issues and to guarantee desirable flight qualities over a large flight envelope [4] [5].

In the following sections, the paper provides information on the initial concept, the STRATOFLY MR3, and the derived concept (Mach 5 MR5 vehicle). The methodology used to redesign the flight control surfaces is then presented, together with the preliminary analysis carried out to verify the vehicle's longitudinal static stability and trim. Eventually, conclusions are reported and a focus on the required future works is also presented.

2. Case studies

2.1. Reference vehicle: STRATOFLY MR3

The STRATOFLY MR3 ([4], [6]) is a highly integrated aircraft designed for Mach 8 flight. An overview of the entire vehicle is reported in Fig. 1, while its main data are shown in Table 1. It adopts a waverider configuration to maximize aerodynamic efficiency (L/D) during hypersonic cruise. This aircraft is powered by a combination of six Air-Turbo-Rocket engines and one Dual-Mode Ramjet engine. Liquid hydrogen serves as the propellant, stored in integrated cryogenic bubble tanks. The primary advantage of this type of propellant lies in its high specific energy, which allows to cover antipodal routes at Mach 8, while ensuring no CO₂ emissions. The typical mission profile covers antipodal routes spanning up to 19000 km in approximately 3-3.5 hours. The STRATOFLY MR3 vehicle is equipped with a fully movable canard, 4 elevons, 2 body-flaps on top of the integrated nozzles and a pair of V-shaped rudders, as can be seen in Fig. 2.



Fig. 1 STRATOFLY MR3

Table 1. STRATOFLY MR3 data

Parameter	Value
Length [m]	94
Wingspan [m]	41
Total plan area [m ²]	2491
Reference range [km]	19000
MTOM [Mg]	400
Fuel mass [Mg]	180

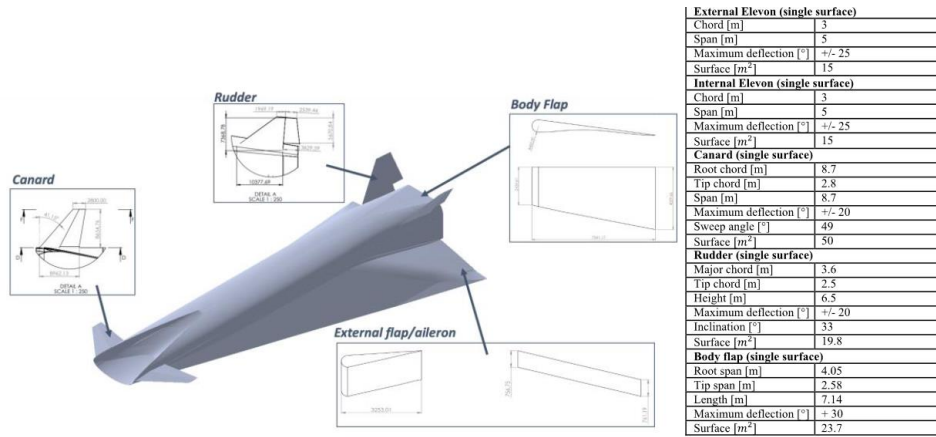


Fig. 2 STRATOFly MR3 Flight Control Surfaces [6]

2.2. MR5 vehicle

As mentioned earlier, the MR5 concept serves as a civil passenger aircraft designed to cruise at Mach 5, and it has been selected as a case study for the H2020 MORE&LESS project. The design of this concept draws upon the findings of the STRATOFly MR3, which demonstrated exceptional efficiency and operational capabilities at Mach 8. A comprehensive description of the methodology used for the aircraft's redesign can be found in [7].

Given these initial findings and the necessity to design a vehicle optimized for the Mach 5 cruise, it became evident that a scaling process was necessary to reduce the total dimension of the reference vehicle. Two potential approaches were initially considered: homogeneous scaling and 1D scaling. In the first approach, the original MR3 layout remains unchanged in terms of proportions, but overall dimensions are reduced. This approach offers advantages such as consistent aerodynamic performance, but the available volume reduces significantly. Then, the 1D scaling was selected. It generates a different configuration with reduced slenderness, as the length reduction is proportionate across the aircraft. A factor of 0.80 is selected to reduce the aircraft length with respect to the reference MR3 configuration. An overview of the vehicle is reported in Fig. 3, while its main data are found in Table 2.

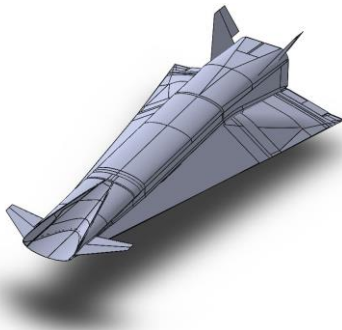


Fig. 3 MR5 vehicle

Table 2. MR5 vehicle data

Parameter	Value
Length [m]	75
Wingspan [m]	41
Total plan area [m ²]	2000
Reference range [km]	19000
MTOM [Mg]	288.4
Fuel mass [Mg]	112.0

3. Methodology

The first step in the definition of MR5's flight control system deals with the sizing of control surfaces. The same type and number of control surfaces of the STRATOFly MR3 vehicle are considered. Two possibilities can be analyzed to complete the scaling process of each control surface: linear or homogeneous scaling. However, since the main vehicle has been scaled according to a linear law, the same approach is followed also for the control surfaces.

The canard sizing is carried out exploiting the tail design method by Sadraey [8]. It is based on the surface volume coefficient, which is expressed as:

$$V_c = \frac{S_c \cdot l_c}{S_{ref} \cdot MAC} \quad (1)$$

Where S_c is the canard plan surface, l_c is the arm of the canard, S_{ref} is the wing reference surface, and MAC is the wing main aerodynamic chord. First, the canard volume coefficient of the MR5 vehicle is kept equal to the one of the MR3 vehicle. Moreover, l_c is also derived from the MR3 case, considering the scaling factor of 0.80. The resulting canard plan surfaces can be evaluated considering that:

$$V_{cMR5} = V_{cMR3} \rightarrow \frac{S_{cMR3} \cdot l_{cMR3}}{S_{refMR3} \cdot MAC_{MR3}} = \frac{S_{cMR5} \cdot (0.80 \cdot l_{cMR3})}{S_{refMR5} \cdot MAC_{MR5}} \quad (2)$$

The canard sweep angle Λ_c , taper ratio λ_c and aspect ratio AR_c are equal to the ones of MR3 vehicle. Then, it is possible to evaluate the remaining geometrical parameters, such as span b_c , root chord c_{rc} and tip chords c_{tc} :

$$b_c = \sqrt{S_c \cdot AR_c} \quad (3)$$

$$c_{rc} = \frac{2 \cdot S_c}{b_c \cdot (1 + \lambda_c)} \quad (4)$$

$$c_{tc} = c_{rc} \cdot \lambda_c \quad (5)$$

The elevons are designed considering the ratio between the surface of the mobile part and the total wing plan surface. It assumed that this ratio remains constant with respect to the one of the MR3 vehicle. The same approach is also used for the body-flap sizing.

Once the control surfaces are defined, the aircraft longitudinal static stability can be analyzed. During a typical mission, high-speed vehicles fly through very different flight regimes and the aerodynamic center position varies accordingly, which can cause instability problems. The longitudinal static stability condition is given by Eq. 6:

$$\frac{\delta C_{M_y}}{\delta \alpha} < 0 \quad (6)$$

Where δC_{M_y} is the derivative of the pitching moment coefficient C_{M_y} and α is the angle of attack. C_{M_y} depends on the relative position of the center of gravity x_{CoG} and the aerodynamic center x_{ac} :

$$C_{M_y} = C_z \frac{x_{CoG} - x_{ac}}{MAC} \quad (7)$$

Once the static stability is verified, the focus shifts on the analysis of trim conditions. A simplified approach is adopted, assuming that the lift and thrust can always balance the weight and drag of the aircraft and focusing solely on achieving rotational equilibrium around the center of gravity. The pitching moment coefficient is evaluated as the sum of several contribution:

$$C_{M_y} = C_{M_{clean}} + \Delta C_{M_{canard}} + \Delta C_{M_{elevon}} + \Delta C_{M_{bodyflap}} = 0 \quad (8)$$

Where:

- $C_{M_{clean}}$ is the pitching moment coefficient of the clean configuration, which consists of the external vehicle layout including empennages and undeflected control surfaces.
- $\Delta C_{M_{canard}}$ is the contribution to the pitching moment coefficient due to the deflection of canards.
- $\Delta C_{M_{elevon}}$ is the contribution to the pitching moment coefficient due to the deflection of elevons.
- $\Delta C_{M_{bodyflap}}$ is the contribution to the pitching moment coefficient due to the deflection of the bodyflap.

The aerodynamic data of the clean configuration has been evaluated through inviscid CFD simulations, and viscous effects have been added exploiting a simplified engineering formulation [9], which has been previously developed for the STRATOFly MR3 vehicle [4].

However, the aerodynamic characterization of the control surfaces has not started yet. For that reason, there is the need for a simplified approach to preliminary evaluate the main characteristics of newly

defined control surfaces, prior to performing higher fidelity analyses. Hence, the already available aerodynamic data of the STRATOFly MR3 vehicle are exploited to derive the possible behavior of the new control surfaces of the scaled vehicle. The normal force coefficient curve slope is supposed to vary proportionally to the ratio of the clean coefficient slopes between the scaled and the original vehicle, as shown in Eq. (9). Accordingly, the same procedure is followed to evaluate the pitching moment coefficient.

$$(\Delta C_z)_{MR5} = (\Delta C_{z_0})_{MR3} + (\Delta C_{z_\alpha})_{MR3} \cdot \frac{(C_{z_\alpha})_{MR5}}{(C_{z_\alpha})_{MR3}} \cdot \alpha \quad (9)$$

4. Results

The geometric data of each control surface has been evaluated according to the methodology described in section 3. The resulting canard data are reported in Table 3, together with a plan drawing of the control surface in Fig. 4.

Table 3. Geometric parameters of the canards

Parameter	Value
Canard plan area S_c [m^2]	79.5
Sweep angle Λ_c [deg]	41
Taper ratio λ_c [-]	0.32
Aspect ratio AR_c [-]	3.03
Span b_c [m]	15.51
Root chord c_{rc} [m]	7.75
Tip chord c_{tc} [m]	2.50

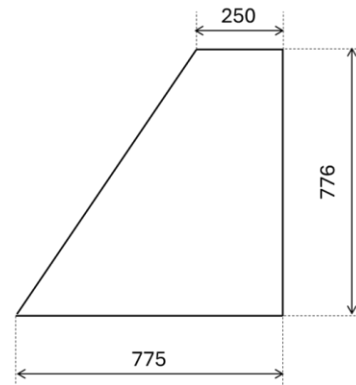


Fig. 4 Plan drawing of the canard (dimensions in mm)

The design of the elevon is based on the ratio between the area of the mobile parts and the total plan area of the reference MR3 vehicle. Then, knowing the total plan area of the MR5 aircraft, the new plan surface of the elevon can be evaluated (Eq. 10). The elevon has a rectangular plan surface, with the same span as the one of the MR3 vehicle.

$$\frac{S_{televonMR3}}{S_{refMR3}} = \frac{S_{televonMR5}}{S_{refMR5}} = 0.024 \rightarrow S_{televonMR5} = 0.024 \cdot S_{refMR5} = 47.98 \text{ m}^2 \quad (10)$$

This procedure is also followed to evaluate the body flap plan surface, which has a trapezoidal shape. The major and minor spans are kept constant and are equal to 4.05m and 2.58m, respectively (Fig. 5).

$$\frac{S_{tbfMR3}}{S_{refMR3}} = \frac{S_{tbfMR5}}{S_{refMR5}} = 0.019 \rightarrow S_{tbfMR5} = 0.019 \cdot S_{refMR5} = 37.9 \text{ m}^2 \quad (11)$$

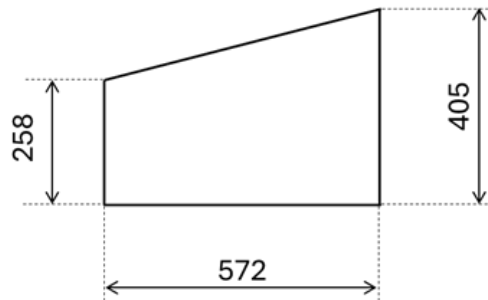


Fig. 5 Body flap geometry (dimensions in mm)

The next step is to analyze the MR5's static longitudinal stability, considering the scaled vehicle and the evaluated control surfaces geometry. First, the aircraft clean configuration is analyzed. The position of the center of gravity is expected to shift between the 56% and the 51% of the vehicle length, as it also happened for the reference STRATOFly MR3 vehicle. As a consequence, the two values of the CoG can be computed:

- $x_{CoG_1} = 42.287 \text{ m}$, which corresponds to the initial position of the CoG, when the aircraft mass is equal to the Maximum Take-Off Mass (MTOM).
- $x_{CoG_2} = 38.298 \text{ m}$, which corresponds to the final position of the CoG where the fuel tanks are empty.

The pitching moment coefficient C_M is evaluated as a function of the angle of attack α at subsonic velocities for the two positions of the center of gravity, as can be seen in Fig. 6. The vehicle shows an unstable behavior for both the CoGs, which suggests that the contribution of control surfaces is required to achieve stability.

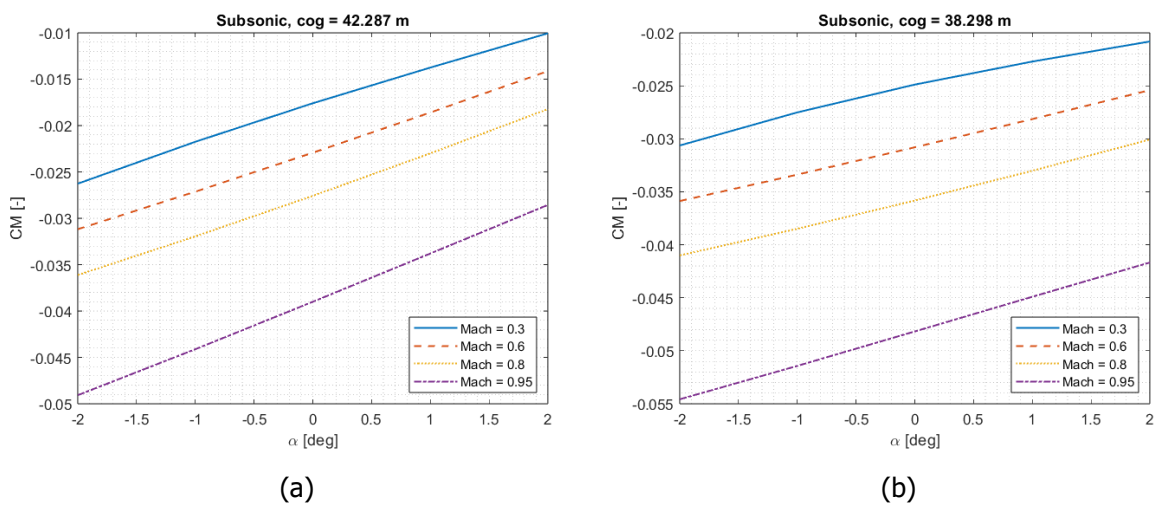


Fig. 6 Clean configuration pitching moment coefficient versus angle of attack at subsonic Mach numbers for the most rearward (a) and forward (b) position of the CoG.

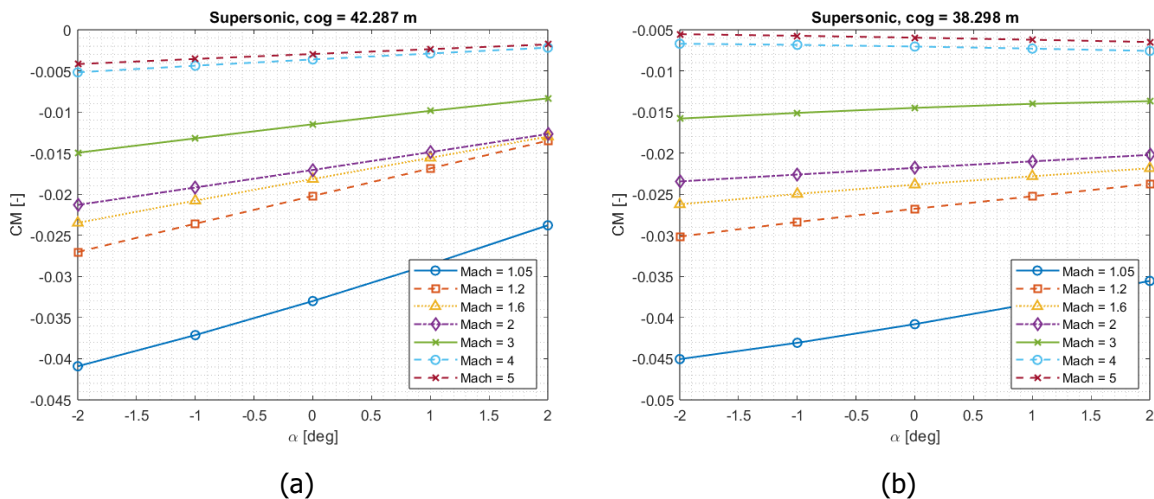


Fig. 7 Clean configuration pitching moment coefficient versus angle of attack at supersonic Mach numbers for the most rearward (a) and forward (b) position of the CoG

Similar trends are also found for Mach numbers greater than 1, as shown in Fig. 7. The only stable conditions are achieved for Mach 4 and Mach 5, and for the most forward position of the CoG (x_{CoG_2}). As expected, control surfaces are necessary to achieve longitudinal stability at different Mach numbers.

If the maximum deflection of the canard ($\delta_{canard} = -20^\circ$) and bodyflap ($\delta_{bodyflap} = -30^\circ$) are considered, the trend of C_{My} becomes negative for the most forward position of the CoG, while it has an almost neutral trend for x_{CoG_1} , as reported in Fig. 8 (a) and Fig. 8 (b).

Slightly better results are found also at Mach 0.8 (Fig. 9), where the trend of the pitching moment coefficient for x_{CoG_2} becomes slightly negative. However, considering that during the initial part of the mission the CoG is predicted to be towards the rearward position x_{CoG_1} , it is clear that the selected control surfaces appear to be not sufficient to achieve stable and trimmed flight at low speed.

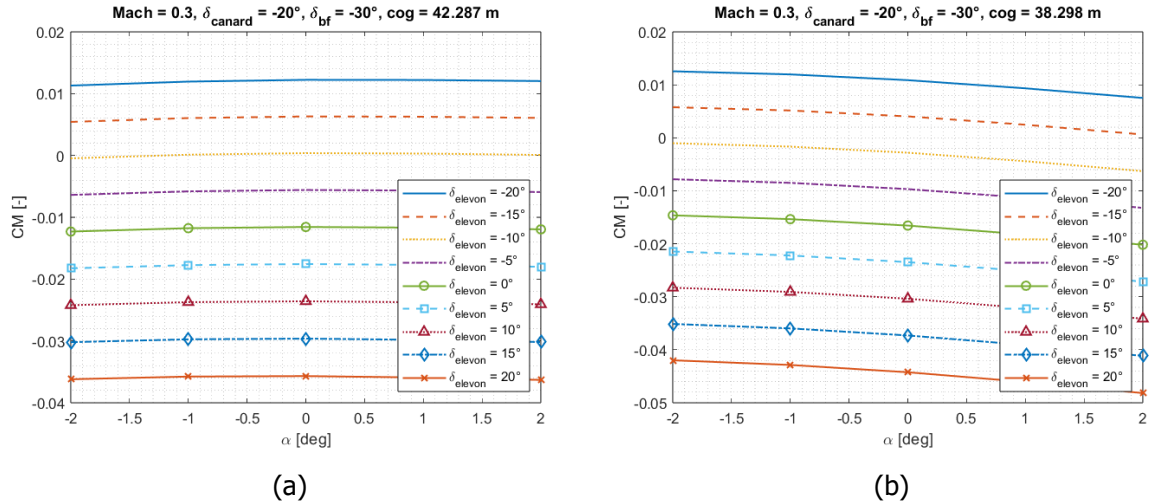


Fig. 8 Pitching moment coefficient versus angle of attack at Mach 0.3, $\delta_{canard} = -20^\circ$ and $\delta_{bf} = -30^\circ$ for different δ_{elevon} , at the most rearward (a) and forward (b) position of the CoG

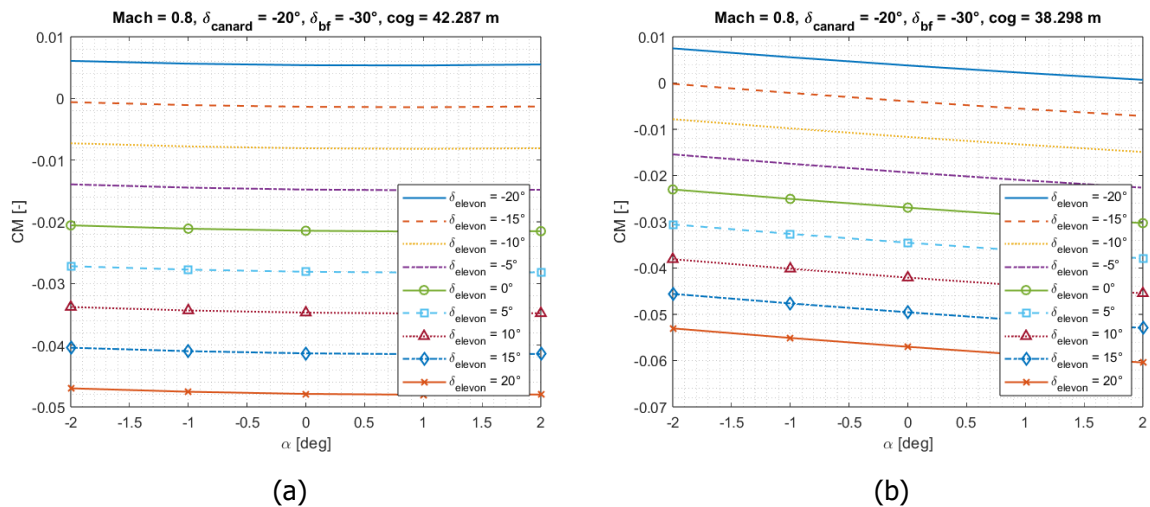


Fig. 9 Pitching moment coefficient versus angle of attack at Mach 0.8, $\delta_{canard} = -20^\circ$ and $\delta_{bf} = -30^\circ$ for different δ_{elevon} , at the most rearward (a) and forward (b) position of the CoG

For this reason, two possible solutions should be further investigated in the next step of the design. First, the control surfaces dimensions should be enlarged, to increase the contribution to the pitching moment coefficient and to contribute to the longitudinal stability. In particular, the bodyflap should be the first control surface to be modified, since it gives the greater contribution to the overall C_{My} due to the fact that it is located at the rear of the vehicle, and it has the longest arm with respect to the CoG.

An initial analysis has been undertaken, exploring the possibility of a 30% increase in the contribution of the bodyflap to the overall pitching moment. This analysis hypothesized a necessary augmentation in surface area to achieve the desired outcome. The results obtained for Mach 0.3 and Mach 0.8 are reported in Fig. 10 (a) and Fig. 10 (b), respectively. The trend of the pitching moment is now negative,

meaning that the vehicle is longitudinally stable if the maximum deflections of the canard and bodyflap and the most rearward CoG position are considered.

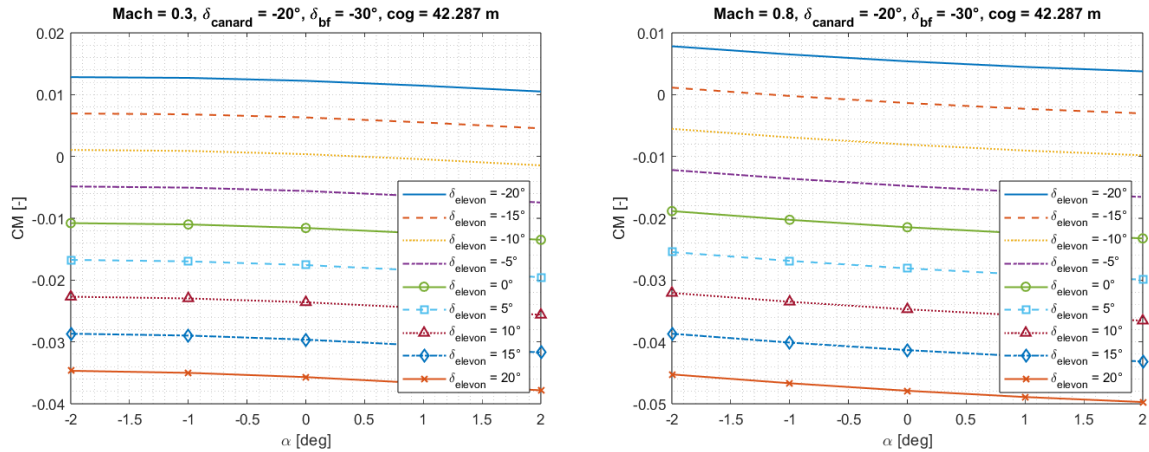


Fig. 10 Pitching moment coefficient vs α for $\delta_{canard} = -20^\circ$, $\delta_{bodyflap} = -30^\circ$, $x_{CoG} = 42.287\text{ m}$ and Mach=0.3 (a) and Mach=0.8 (b)

Moreover, the true position of the CoG at the different Mach number should also be further analyzed, considering the internal subsystem arrangement, the amount of fuel consumed and the depletion strategy to be adopted during the mission. All these aspects have been widely studied during the design of the STRATOFly MR3 vehicle but have not yet started for the Mach 5 configuration. Indeed, the two positions of the CoG considered in the analysis have been selected from the original STRATOFly MR3 vehicle and can be subject to changes.

At Mach 1.2, the trend of the pitching moment coefficient is negative in the entire range of CoGs considered and for the maximum deflection of canard and bodyflap, as can be seen in Fig. 11. These deflections allow to achieve trim conditions in the range of angles of attacks between -2° and $+2^\circ$, depending on the elevon deflection. Moreover, the longitudinal stability and trimmability of the vehicle are verified also for lower deflections of the control surfaces. For example, considering $\delta_{canard} = 0^\circ$, $\delta_{bf} = -30^\circ$ and x_{CoG_1} , trim conditions can be achieved with elevon deflections between -20° and -5° (Fig. 12). Similar results are also obtained for x_{CoG_2} , $\delta_{canard} = -10^\circ$ and $\delta_{bf} = -24^\circ$, as can be seen in Fig. 13.

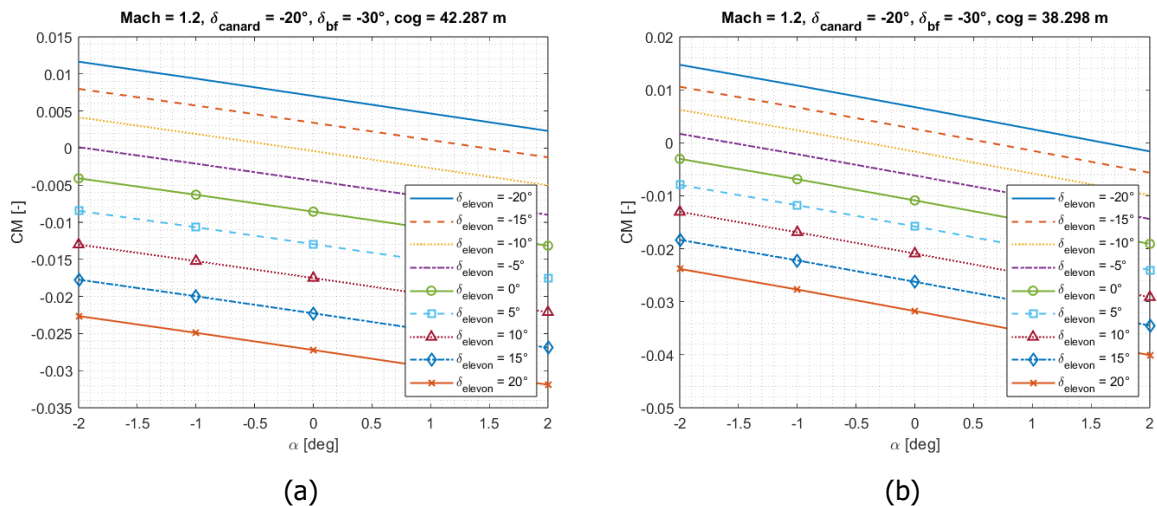


Fig. 11 Pitching moment coefficient versus angle of attack at Mach 1.2, $\delta_{canard} = -20^\circ$ and $\delta_{bf} = -30^\circ$ for different δ_{elevon} , at the most rearward (a) and forward (b) position of the CoG

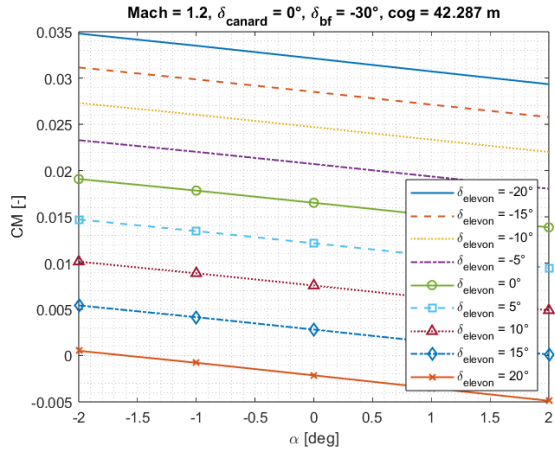


Fig. 12 Pitching moment coefficient versus angle of attack at Mach 1.2, $\delta_{canard} = 0^\circ$ and $\delta_{bf} = -30^\circ$ for different δ_{elevon} , at the most rearward position of the CoG

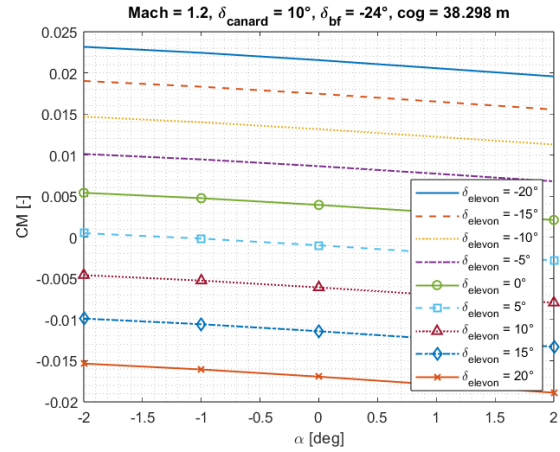
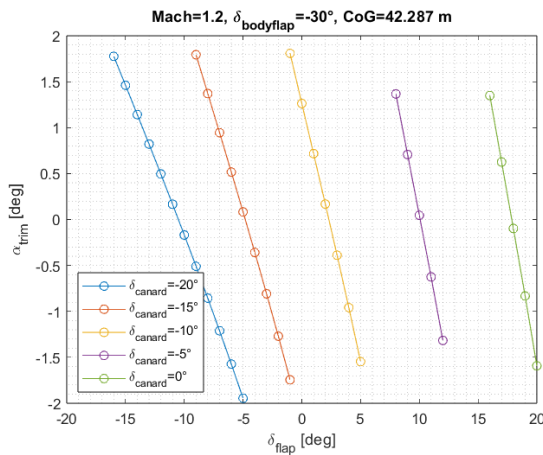
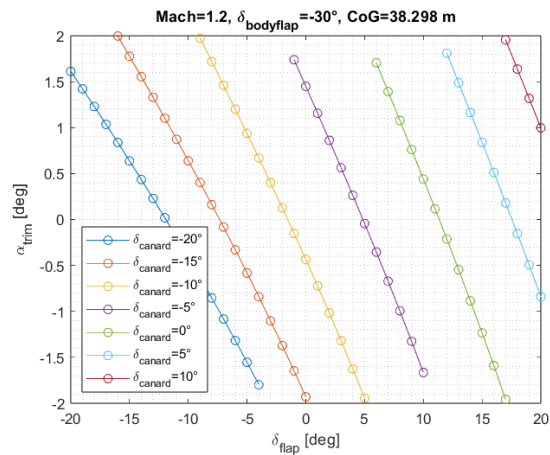


Fig. 13 Pitching moment coefficient versus angle of attack at Mach 1.2, $\delta_{canard} = 10^\circ$ and $\delta_{bf} = -24^\circ$ for different δ_{elevon} , at the most forward position of the CoG

Fig. 14 (a) and Fig. 14 (b) report the computed trim angles for Mach 1.2, $\delta_{bodyflap} = -30^\circ$, for different δ_{canard} and the two position of the center of gravity. It can be seen that the vehicle is longitudinally stable and trimmed for the entire range of angles of attack, considering different combinations of control surfaces deflections.



(a)



(b)

Fig. 14 α_{trim} vs δ_{flap} for Mach=1.2, $\delta_{bodyflap} = -30^\circ$, and different deflections of canards, for the most rearward (a) and forward (b) position of the CoG

Eventually, the vehicle's stability at cruise Mach number equal to 5 is also evaluated. The MR3 vehicle is longitudinally stable if the maximum control surfaces deflections are considered, as can be seen in Fig. 15 (a) and Fig. 15 (b), for the two positions of the CoG.

The same analysis is also performed considering lower deflections, to identify which is the minimum control surfaces angle which guarantees stability. For the most rearward position of the CoG, $\delta_{bodyflap} = -24^\circ$ and $\delta_{canard} = 0^\circ$ are required to achieve stable and trimmed conditions in the range of angles of attack considered, as shown in Fig. 16. Similar results are also found for the most forward position of the CoG, where $\delta_{bodyflap} = -15^\circ$ and $\delta_{canard} = 15^\circ$ are sufficient to guarantee stability, as shown in Fig. 17.

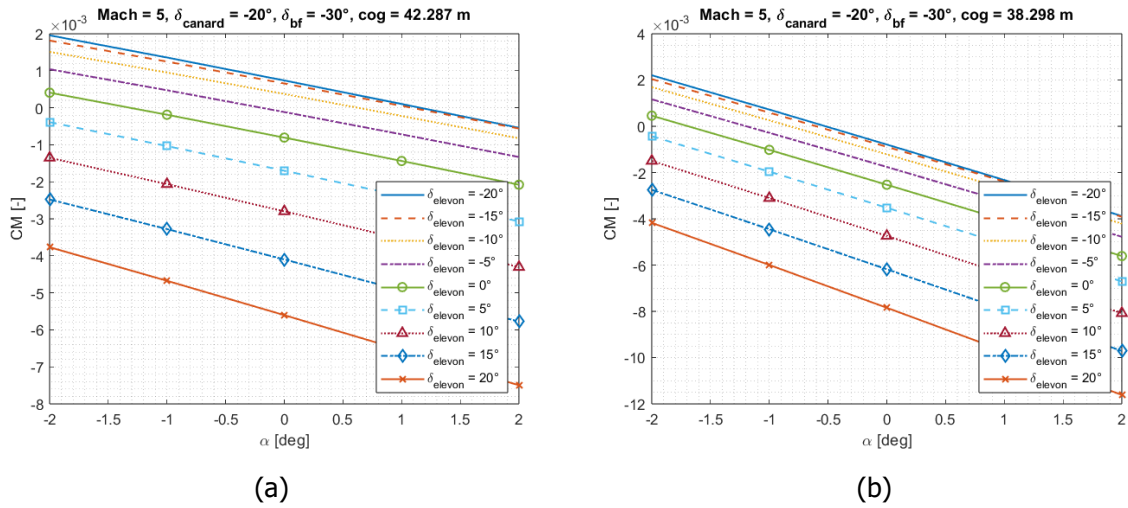


Fig. 15 Pitching moment coefficient versus angle of attack at Mach 5, $\delta_{canard} = -20^\circ$ and $\delta_{bf} = -30^\circ$ for different $\delta_{elevator}$, at the most rearward (a) and forward (b) position of the CoG

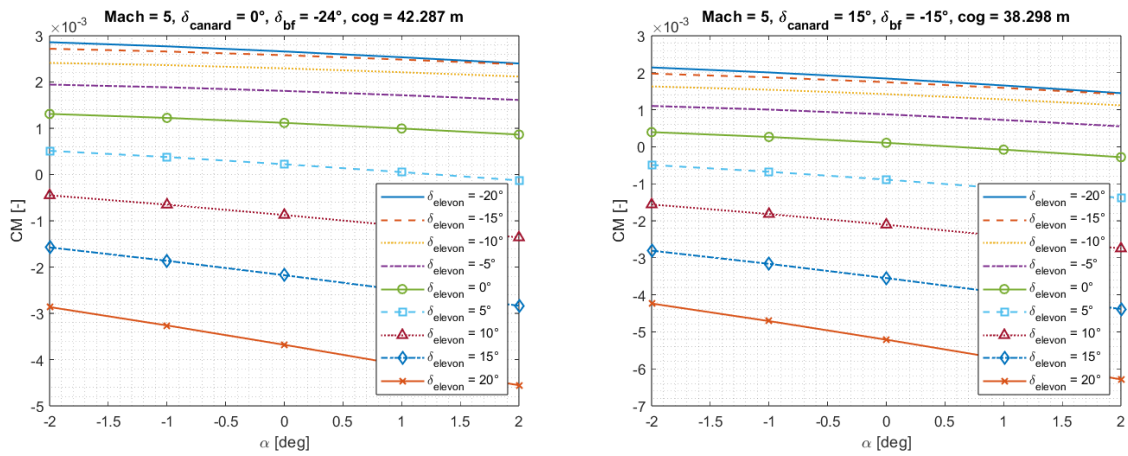


Fig. 16 Pitching moment coefficient versus angle of attack at Mach 5, $\delta_{canard} = 0^\circ$ and $\delta_{bf} = -24^\circ$ for different $\delta_{elevator}$, for the most rearward position of the CoG

Fig. 17 Pitching moment coefficient versus angle of attack at Mach 1.2, $\delta_{canard} = 15^\circ$ and $\delta_{bf} = -15^\circ$ for different $\delta_{elevator}$, for the most forward position of the CoG

An overview of the required deflections to achieve α_{trim} between -2° and $+2^\circ$ is reported in Fig. 18 (a) and Fig. 18 (b), for the two positions of the CoG and for $\delta_{bodyflap} = -30^\circ$. A 3D trim map can be also generated for cruise speed (Mach 5), and for x_{CoG_1} (Fig. 19 (a)) and x_{CoG_2} (Fig. 19 (b)). Each canard deflection is reported with a different color.

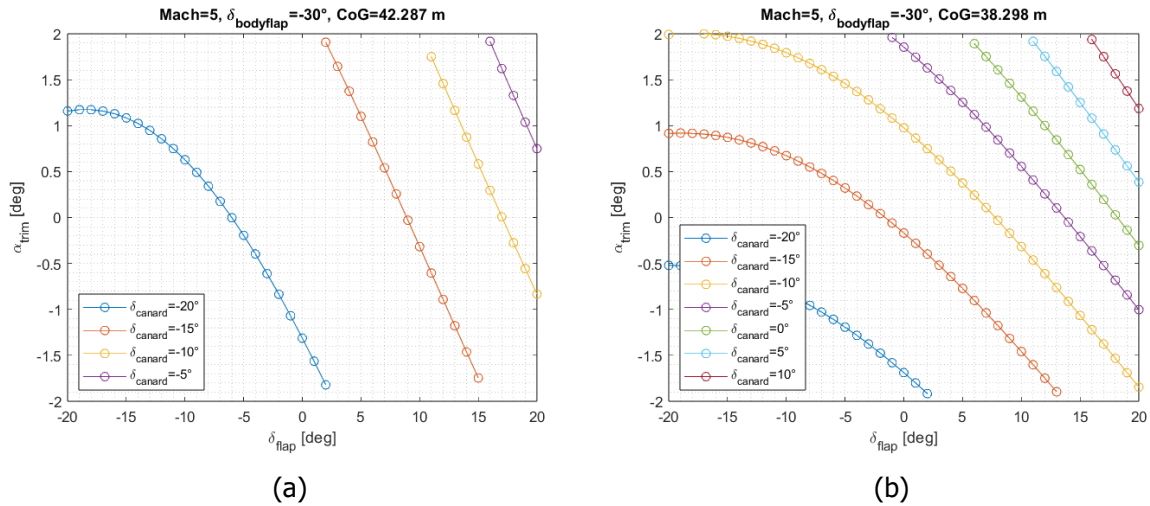


Fig. 18 α_{trim} vs δ_{flap} for Mach=5, $\delta_{bodyflap} = -30^\circ$, and different deflections of canards, for the most rearward (a) and forward (b) position of the CoG

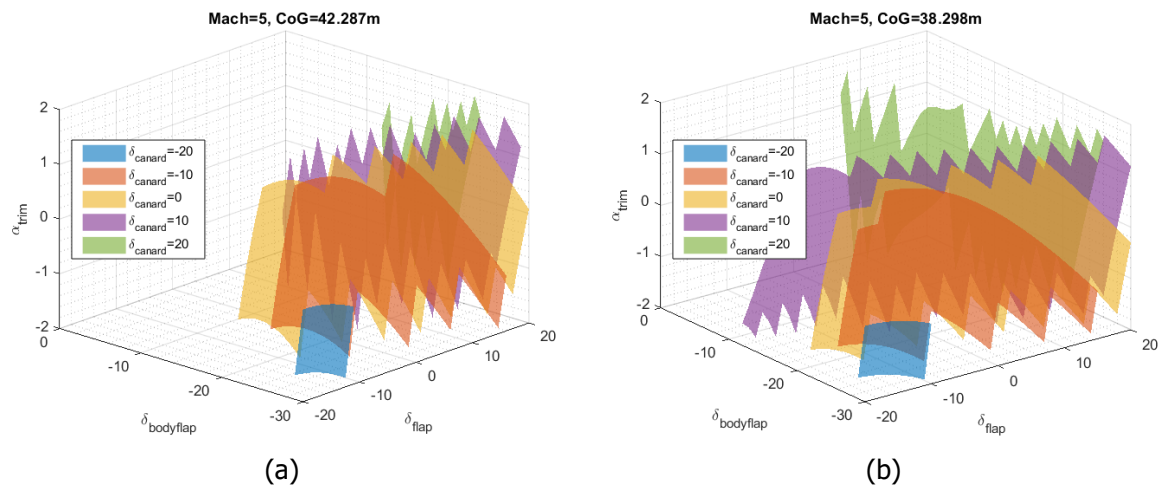


Fig. 19 3D trim maps for Mach=5 and the most rearward (a) and forward (b) position of the CoG

5. Conclusions and future works

This paper reports the preliminary design of the Flight Control System for a Mach 5 waverider, highlighting the significance of considering the FCS from the outset of a project, especially during the initial part of the design phase.

The preliminary design methodology outlined here for the MR5 vehicle demonstrates a systematic approach, beginning with the geometric definition of control surfaces and progressing to estimating necessary deflections for stability and trim across various flight regimes. Since the MR5 waverider is derived from the STRATOFly MR3 vehicle, both these steps are performed exploiting the outcomes of the STRATOFly project, where the aerodynamic and stability performance of the reference vehicle have been evaluated.

First, the longitudinal static stability of the MR5 vehicle has been evaluated considering the clean configuration, where the control surfaces are not deflected. The vehicle is not stable for the entire Mach range, as also happened for the original STRATOFly MR3 vehicle. If the control surfaces are deflected, the vehicle longitudinal static stability is verified for the supersonic Mach range. The trimmed conditions can also be evaluated accordingly.

However, at low speed the maximum deflections of the control surfaces are not sufficient to guarantee stability, if the most rearward position of the CoG is considered. Hence, a further assessment of the control surfaces and a detailed study of the CoG placement is required as a future work.

References

- [1] "<https://www.h2020-stratofly.eu/>," [Online]. [Accessed 21 03 2024].
- [2] "<https://www.h2020moreandless.eu/project/>," [Online]. [Accessed 21 03 2024].
- [3] K. G. Bowcutt, "Physics Drivers of hypersonic Vehicle Design," in *22nd AIAA International Space Planes and Hypersonic Systems and Technology Conference*, Orlando, FL, 2018.
- [4] N. Viola, P. Roncioni, O. Gori and R. Fusaro, "Aerodynamic Characterization of Hypersonic Transportation Systems and Its Impact on Mission Analysis," *Energies*, vol. 14, no. 12, 2021.
- [5] C. C. Coleman and F. A. Faruqi, "On Stability and Control of Hypersonic Vehicles," Weapons Systems Division, DSTO Defence Science and Technology Organisation, Edinburgh, Australia, 2009.
- [6] R. Fusaro, D. Ferretto and N. Viola, "Flight Control System Design and Sizing Methodology for hypersonic cruiser," in *AIAA AVIATION 2022 Forum*, Chicago, IL & Virtual, 2022.
- [7] N. Viola, R. Fusaro, D. Ferretto, O. Gori, M. Marini, P. Roncioni, B. O. Cakir, A. C. Ispir and B. H. Saracoglu, "Hypersonic aircraft and mission concept re-design to move from Mach 8 to Mah 5 operations," in *33rd Congress of the International Council of the Aeronautical Sciences*, Stockholm, Sweden, 2022.
- [8] M. H. Sadraey, *Aircraft Design: A Systems Engineering Approach*, John Wiley & Sons, 2012.
- [9] O. Gori, V. Borio, N. Viola, P. Roncioni, M. Marini, D. Pepelea and M. G. Stoican, "From conceptual to preliminary design: Aerodynamic characterization of MR5 civil high-speed aircraft," in *25th AIAA International Space Planes and Hypersonic Systems and Technologies Conference*, Bengaluru, Karnataka, India, 2023.